S1 Supplemental Materials and Methods

a) Confocal single molecule setup

spFRET experiments were performed on an inverted microscope (Olympus IX70) that was equipped with home-built confocal excitation and detection optics (1). A schematic view of the setup is shown in Figure S1. The donor dye was excited with the 488 nm line of a continuous-wave Ar^+/Kr^+-laser (Melles Griot); donor and acceptor emission was detected in epifluorescence. Fluorescence was separated from scattered laser light by a dichroic beam splitter (505DRLP) and imaged onto a 100 µm pinhole, which rejected any out-of-focus light and defined an effective observation volume of about 1 fL. Transmitted fluorescence was split into two detection channels (donor signal: 500-540 nm, acceptor signal 610-700 nm) defined by an infrared blocking filter (700CFSP), a dichroic beam splitter (580DRLP) and appropriate interference filters (donor channel: 520DF40, transfer channel: 610ALP, all filters and dichroic beam splitters from Omega Optical). A lens in front of each detector focused the fluorescence onto the active area of an avalanche photodiode (SPAD-AQ-14, Perkin-Elmer). The detector signal was read out by a TCSPC board (TimeHarp200, Picoquant GmbH) and processed by our own software which identified and analyzed single molecule events as described in (1).

b) Microplate scanning FRET (µpsFRET)

A variable mode scanner (Typhoon 9400, GE Healthcare) was used to measure the proximity ratio of samples in 384-well microplates (SensoPlate Plus, Greiner Bio-One). A laser spot with a diameter of a few µm (the exact operation parameters were not provided by the manufacturer) was rapidly scanned over the sample array. All images were acquired with a pixel resolution of 100 µm with the image plane set to a height of 3 mm above the scanner surface, which placed the focus inside the microplate chambers. Fluorescence was recorded on two photomultiplier tubes (PMT) with voltages and filter settings as follows:

- donor channel: excitation at 488 nm, detection at 500-540 nm; PMT voltage 625 V.
- acceptor channel: excitation at 532 nm, detection at 595-625 nm; PMT voltage 675 V.
- transfer channel: excitation at 488 nm, detection at 595-625 nm, PMT voltage 675 V.

c) Intensity correction for background, crosstalk and direct excitation

In µpsFRET and spFRET, P is estimated from measured donor and acceptor raw intensities I^0_D and I^0_T. These contain additional contributions from background (B_D and B_T), donor crosstalk into the acceptor channel (α_{DT}) and direct excitation of the acceptor dye (f_{dir}), which have to be corrected for, before a proximity ratio P can be calculated according to equation 2.

$$I_T = \left(I_T^0 - B_T\right) - \alpha_{DT}\left(I_D^0 - B_D\right) - f_{dir}$$
$$I_D = \left(I_D^0 - B_D\right) \quad . \qquad \text{(S1)}$$

Background

In µpsFRET the average background signal per well, B_D and B_T, is measured in one or more separate wells containing pure buffer solution. In spFRET an average count rate of background photons is measured for the buffer solution, yielding photon rates b_D and b_T in units of photons

per millisecond. For the i-th single molecule event b_D and b_T are then multiplied with the duration of the i-th burst, d^i:

$$B_{D,T}{}^{i} = b_{D,T} \cdot d^{i} . \qquad \text{(S2)}$$

Crosstalk of donor emission into the acceptor channel

In µpsFRET one or more wells are filled with a donor-only sample and measured in parallel to double-labeled FRET samples. From the respective intensities in the donor and acceptor channel upon excitation with 488 nm, $I_{Dex}{}^{Dem}$ and $I_{Dex}{}^{Aem}$, we obtain the crosstalk factor as

$$\alpha_{DT} = \frac{I_{Dex}^{Aem} - B_T}{I_{Dex}^{Dem} - B_D} . \qquad \text{(S3)}$$

In spFRET the donor-only sample was measured for 5-10 minutes to build a histogram of the proximity ratio P, equation 2. After background subtraction, the peak value in the P histogram, $P_{D\text{-only}}$, yields the crosstalk factor as

$$\alpha_{DT} = \left(\frac{1}{1/P_{D-only} - 1} \right)^{-1} . \qquad \text{(S4)}$$

Alternatively, α_{DT} can be directly estimated from ahistogram of the burst-wise ratio of background-corrected photon numbers in both channels, analogous to equation S3.

Direct excitation of the acceptor dye

In µpsFRET f_{dir} is determined with an additional measurement of an acceptor-only sample. Acceptor-only and FRET samples are probed with two excitation wavelengths; excitation with 532 nm selectively excites the acceptor, yielding acceptor intensities $(I_{Aex}{}^{Aem})_{A\text{-only}}$ and $(I_{Aex}{}^{Aem})_{FRET}$, while excitation with 488 nm preferentially excites the donor dye, yielding intensities $(I_{Dex}{}^{Aem})_{A\text{-only}}$ and $(I_{Dex}{}^{Aem})_{FRET}$for the acceptor-only and FRET sample.

After background correction the only contribution to $(I_{Dex}{}^{Aem})_{A\text{-only}}$ comes from direct acceptor excitation and we can define a ratio

$$S_A = \frac{\left(I_{Dex}^{Aem} - B_T\right)_{A-only}}{\left(I_{Aex}^{Aem} - B_A\right)_{A-only}} . \qquad \text{(S5)}$$

S_A is expected to be the same for acceptor molecules in the FRET-active sample and in the acceptor-only sample. Based on the measured intensity $(I_{Aex}{}^{Aem})_{FRET}$, we then obtain the contribution of direct excitation in the FRET sample as

$$f_{dir} = S_A \cdot \left(I_{Aex}^{Aem} - B_A\right)_{FRET} . \qquad \text{(S6)}$$

In one-color spFRET f_{dir} is estimated based on the number of detected photons in the donor channel, I_D. For a known detection factor γ and energy transfer E; the number of photons due to direct acceptor excitation is given as

$$f_{dir} = \frac{\varepsilon_A}{\varepsilon_D} \cdot \frac{I_D \gamma}{(1-E)} , \qquad \text{(S7)}$$

where ε_A and ε_D denote the extinction coefficient of acceptor and donor dye at 488 nm. For our system $\varepsilon_A/\varepsilon_D \approx 0.043$ and $\gamma \approx 1.7$.

d) Primer sequences used for the preparation of labeled DNA fragments.

All primers were purchased from IBA Germany and used without further purification.

Internally labeled DNA:

5'-ACCCTATACGCGGCCCTGGAGAATCCCGGTG-CCGAAACCGC**T(Alexa488)**CAATTG-3'

5'-CATGCACAGGATGTATATATCTGACACGTG-CC**T(Alexa594)**GGAGAC-3'.

Linker DNA labeled DNA:

5'-**G(Alexa488)**GACCCTATACGCGGCC-3'

5'-**T(Alexa594)**GCACAGGATGTATATATCTGAC-3'.

e) cleaning procedure for 384-well microplates

Before each set of experiments, the microplates were cleaned by soaking in 1% Hellmanex solution (Hellma) for 30 minutes twice, with thorough washing with ddH_2O in between. The wells were then treated with 100 mM HCl for 30 minutes and cleaned with ddH_2O. After repeating the acid treatment at least once, microplates were dried on a heating block ($T < 40°C$) and/or under low vacuume. To passivate the surface, each well was filled with Sigmacote™ solution, incubated for 15-20 seconds and blocked with ddH_2O. After all wells were treated with Sigmacote the microplate was thoroughly rinsed with ddH_2O and dried on the heating block. Passivated plates were then sealed with film (Bio-Rad) to avoid exposure to dust and stored for subsequent use.

S2 Statistical analysis of spFRET distributions

To describe the salt-dependent nucleosome heterogeneity we first selected the relevant bursts and analyzed the statistical moments of the respective subpopulation. These provide an efficient, phenomenological means to locate changes in position and shape of the distribution without the need for a priori estimation of the exact number of substates involved.

a) Simulations

To learn more about the properties of the distribution moments we first simulated a mixture of two FRET species that mimicked the heterogeneity observed in spFRET P_{FRET} was approximated by two populations at $P_A \approx 0.4$ and $P_B \approx 0.55$ with identical standard deviation of $\sigma_P = 0.08$: we found that these parameters provided a decent approximation to the experimental data. The ratio between states A and B was varied from 100% species A to 100% species B to mimic transition of molecules from state A to state B. For each A:B ratio we simulated 10 different distributions with 2000 events $\{P_i\}$ each and computed the first four distribution moments (mean value, variance, skewness and kurtosis), which are defined as follows:

Mean value: $$\langle P \rangle = \frac{1}{N}\sum_{i=1}^{N} P_i \qquad \text{(S8)}$$

Variance: $$\sigma_P^2 = \frac{1}{N-1}\sum_{i=1}^{N}\left(P_i - \langle P \rangle\right)^2 \qquad \text{(S9)}$$

Skewness: $S_P = \frac{1}{N}\sum_{i=1}^{N-1}\left(\frac{P_i - \langle P\rangle}{\sigma_P}\right)^3$ (S10)

Kurtosis: $K_P = \frac{1}{N}\sum_{i=1}^{N-1}\left(\frac{P_i - \langle P\rangle}{\sigma_P}\right)^4 - 3$ (S11)

All simulations were done using built-in functions of IGOR Pro (WaveMetrics). Average value and standard error of each parameter from 10 simulations are shown in Figure S7. As molecules transit from state A to state B, each moment changes in a characteristic pattern: 1) the mean value increases linearly as more molecules are in state B. 2) population of state B results in an increase in variance until both species are equally present and the net distribution is broadest. As state B starts to dominate the variance decreases again. 3) At 100% species A the distribution is symmetric and the skewness equals zero. A maximum in skewness is reached for a certain percentage of species B (where the distribution is most asymmetric) followed by a characteristic, quasi linear decrease as the distribution becomes more symmetric. At equal proportions of states A and B the skewness is zero, while the variance is maximal. As species B starts to dominate the skewness parameter reverses sign and undergoes a negative maximum before returning to zero for 100% species B. 4) Last, the kurtosis undergoes a more complex change with multiple transits through zero and rather sharp changes in between.
The change in mean value and skewness appear most suitable for analysis, as they provide a linear readout in an extended range of the transition (between 20% and 80% state B).

b) Calculation of experimental distribution moments

To compute mean value and skewness for the experimental data we first isolated the nucleosome subpopulation by subtracting the contribution of donor-only and free DNA from the histogram. To do so, a double Gaussian was approximated to the first part (P<0.2) of each P distribution (see Figure S8A). Center position and width of each Gaussian were determined from independent histograms of a donor-only sample and the DNA distribution observed at 1200 mM NaCl where practically all nucleosomes were dissociated.
Next, the net nucleosome distribution, $P_{FRET} = P_{full} - P_{D\text{-}only} - P_{DNA}$ was used to calculate a weighting factor $f = P_{FRET}/P_{full}$ for each proximity ratio interval [P, P+dP], where dP is the bin width in the histogram, usually set to 0.02. An exemplary distribution of the weighting factor f is shown in the lower half of Figure S8A. f_i represents the fraction of molecules with $P_i < P < P_i+dP$ that contribute to the FRET population (nucleosome population).
We then computed the mean value and skewness of P_{FRET} as a function of salt concentration using IGOR Pro software. The range of analyzed P-values was limited to values less than 0.85 (to exclude acceptor only events) and a lower limit P_{min}, which we defined as the proximity ratio, from which on the cumulative sum of P_{FRET} is always positive. In other words, the number of events with $P < P_{min}$ in the histogram equals the number of events in the fitted D-only and DNA population. The subsequent analysis of the salt-dependence of mean value and skewness is reported in the manuscript.

S3: Sequences of histone fragments

The level of acetylation in C- and N-terminal fragments were analyzed by MALDI-TOF. The center region was not amenable to sequencing.

Histone H2A:

N-terminus (47 AA)	SGRGKQGGKTRAKAKTRSSRAGLQFPVGRVHRLLRKGNYAERVGAGA
Center region (32 AA)	PVYLAAVLEYLTAEILELAGNAARDNKKTRII
C-terminus (50 AA)	PRHLQLAVRNDEELNKLLGRVTIAQGGVLPNIQSVLLPKKTESSKSAKSK

Histone H2B:

N-terminus (44 AA)	AKSAPAPKKGSKKAVTKTQKKDGKKRRKTRKESYAIYVYKVLKQ
Center region (34 AA)	VHPDTGISSKAMSIMNSFVNDVFERIAGEASRLA
C-terminus (44 AA)	HYNKRSTITSREIQTAVRLLLPGELAKHAVSEGTKAVTKYTSAK

Histone H3:

N-terminus (45 AA)	ARTKQTARKSTGGKAPRKQLATKAARKSAPATGGVKKPHRYRPGT
Center region (55 AA)	VALREIRRYQKSTELLIRKLPFQRLVREIAQDFKTDLRFQSSAVMALQEASEAYL
C-terminus (35 AA)	VALFEDTNLCAIHAKRVTIMPKDIQLARRIRGERA

Histone H4:

N-terminus (45 AA)	SGRGKGGKGLGKGGAKRHRKVLRDNIQGITKPAIRRLARRGGVKR
Center region (31 AA)	ISGLIYEETRGVLKVFLENVIRDAVTYTEHA
C-terminus (26 AA)	KRKTVTAMDVVYALKRQGRTLYGFGG

References

1. Gansen, A., A. R. Hieb, V. Böhm, K. Tóth, and J. Langowski. 2013. Closing the Gap between Single Molecule and Bulk FRET Analysis of Nucleosomes. PLoS One 8:e57018.
2. Suckau D. and A. Resemann. 2009. MALDI Top-Down Sequencing: Calling N- and C-Terminal Sequences with High Confidence and Speed. J. Biomol Tech **20**(5), 258-262

Supplemental Tables

Table S1

The extent of chemical acetylation per histone was analyzed with MALDI-TOF (T3 sequencing) (2) and supplemental Edman sequencing. Amino acid sequences of the C- and N-terminal fragments that were analyzed are listed in supplemental section S3, along with the central AA sequence that was not amenable to sequencing, For the N-terminal and C-terminal region the table lists the number of analyzed amino acids ($N_{analyzed}$), the total number of lysines present ($N_{lys,\ total}$) and the number of detected acetylated lysines ($N_{lys,\ acet}$). The last two columns list the number of central residues and lysines within that were not analyzed. For example, for the N-terminus of H3 "0 - 3(4)" means, that we found 0, 1, 2 and 3 lysines that were acetylated (single or multiple). We also found some molecules that had a 4-th acetylated lysine, but with a small degree of acetylation. These data confirm that the majority of acetylation occurred at the N-termini of the proteins.

We note that by T3 sequencing we found that H4K91, located in the C-terminal region of histone H4, was acetylated in all our samples. Since we detected no other acetylated lysines in the C-terminal region of H4, we can conclude that H4K77 and H4K79 were not acetylated. Another important biological acetylation site, H3K56 is located in the central part of histone H3, which was not amenable to T3 sequencing. We cannot exclude that H43K56 was acetylated in some octamers, but based on the overall level of acetylation of H3 we estimate that this was the case in maybe 30% of all octamers.

	N-terminus			C-terminus			Center region	
Histone	$N_{analyzed}$	$N_{lys,\ total}$	$N_{lys,\ acet}$	$N_{analyzed}$	$N_{lys,\ total}$	$N_{lys,\ acet}$	N_{missed}	$N_{lys,missed}$
H2A	47	5	0 – 3	50	6	0 - 1(2)	32	2
H2B	44	12	0 – 3	44	5	0 - 1	34	1
H3	45	8	0 - 3(4)	35	2	0 (1)	55	3
H4	45	7	0 - 3	26	3	1	31	1

Supplemental Figures

Figure S1

Experimental setup for spFRET and µpsFRET experiments: **A**) Confocal detection of diffusing molecules in 384-well microplates. Abbreviations: DM: dichroic mirror, F: emission filter, APD: avalanche photodiode, PMT, photomultiplier tube, PH: pinhole. **B**) Single molecule analysis of nucleosomes. The passage of individual nucleosomes through the focus generates bursts of fluorescence. For each burst a proximity ratio is calculated and data binned for histogram analysis. **C)** Microplate-scanning FRET (µpsFRET) analysis of nucleosome stability. Samples are imaged in three spectral channels on a Typhoon™ multimode scanner. From the intensities in donor, acceptor and transfer channel proximity ratios are calculated for each well. The salt-dependent proximity ratio is then approximated by a sigmoidal function to quantify nucleosome stability.

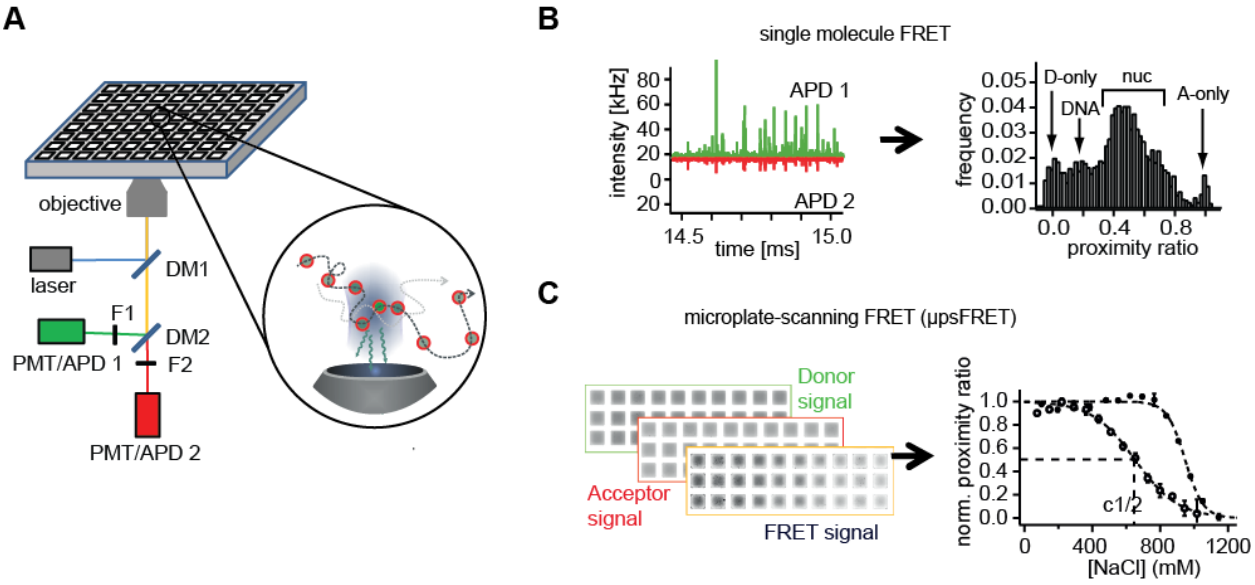

Figure S2

Dilution series of non-acetylated nucleosomes at 150 mM NaCl: **A**) exemplary spFRET histogram at 250 pM nucleosomes (50 pM labeled and 200 pM unlabeled dl-I nucleosomes). D-only and DNA subpopulations were approximated by two Gaussians and subtracted from the measured P distribution to yield the nucleosome subpopulation ("Nuc", thick black line in Fig S2A). **B**) fraction of intact nucleosomes ("Nuc"/("DNA"+"Nuc")) as a function of total nucleosome concentration. Samples are stable at 300 pM, the concentration used for FRET experiments. Dissociation due to mass action was observed at nucleosome concentrations smaller than 50 pM.

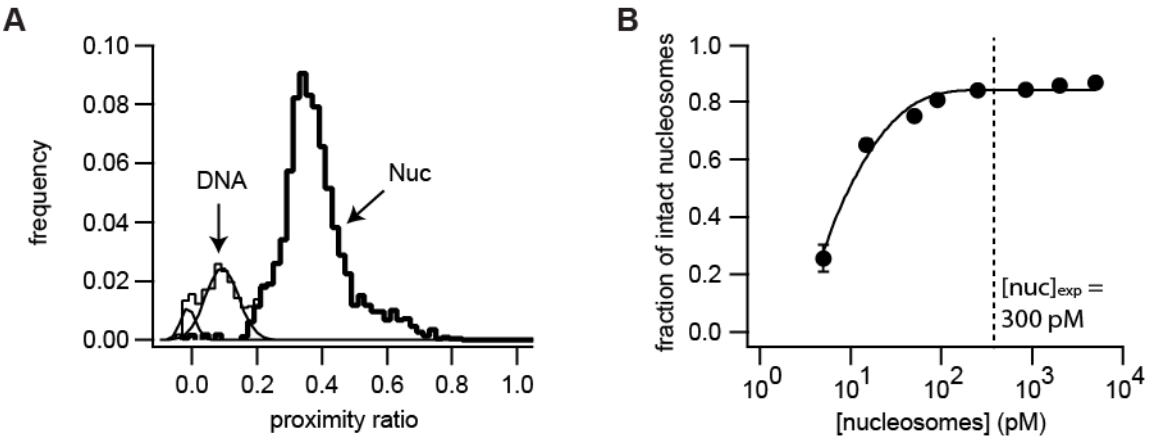

Figure S3

Salt titration curves for end-labeled (**A**) and internally labeled nucleosomes (**B**) at 300 pM (open circles) and 3 nM (solid circles) nucleosome concentration. $c_{1/2}$ values were determined from a sigmoidal fit to data. (A) end-labeled nucleosomes (dl-E): $c_{1/2}$ = (676 ± 35) mM (300 pM) and $c_{1/2}$ = (682 ± 25) mM (3 nM). (B) internally labeled nucleosomes (dl-I): $c_{1/2}$ = (952 ± 8) mM (300 pM) and $c_{1/2}$ = (1025 ± 10) mM (3 nM), Loss of dl-E FRET was concentration-independent ($\Delta c_{1/2}$ < 1%), suggesting that reversible unwrapping at the DNA ends dominates the FRET signal rather than disassembly. FRET in dl-I nucleosomes was concentration-dependent ($\Delta c_{1/2}$ > 7%), suggesting that it reports on gross nucleosome disassembly.

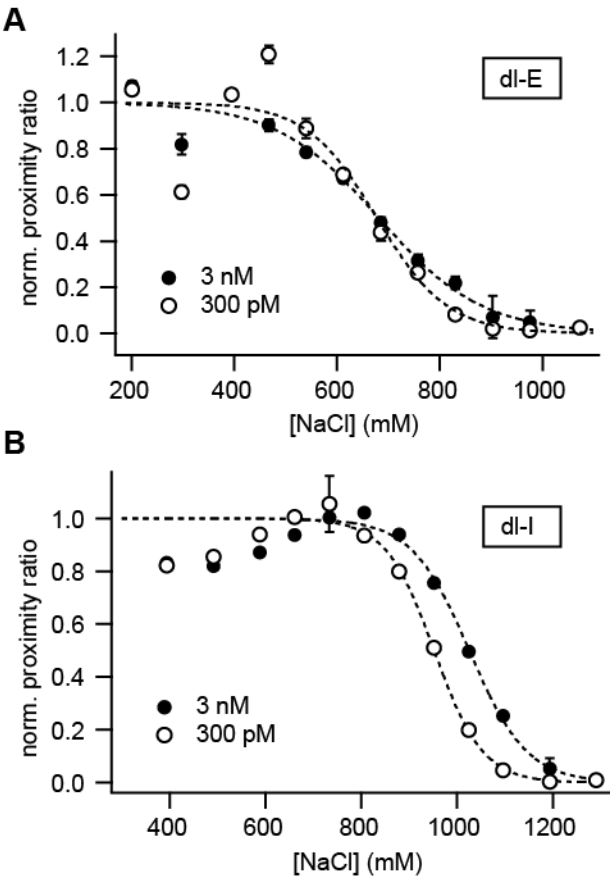

Figure S4

Non-normalized µpsFRET data from end-labeled nucleosomes (dl-E) between 0 mM and 500 mM NaCl (3 independent salt titrations each): At physiological ionic strength measured proximity ratios of non-acetylated and H4-acetylated nucleosomes are very similar and significantly higher (≈ 30 %) than those of H3-acetylated and H3/H4-acetylated constructs. This suggests that H4-acetylation does not affect linker DNA geometry below 300-400 mM NaCl and that at low salt nucleosome opening is dominated by acetylation of histone H3. At higher ionic strength the different acetylated constructs show a stronger loss in FRET than non-acetylated nucleosomes, which eventually lead to the differences in $c_{1/2}$ that are reported in Figure 2.

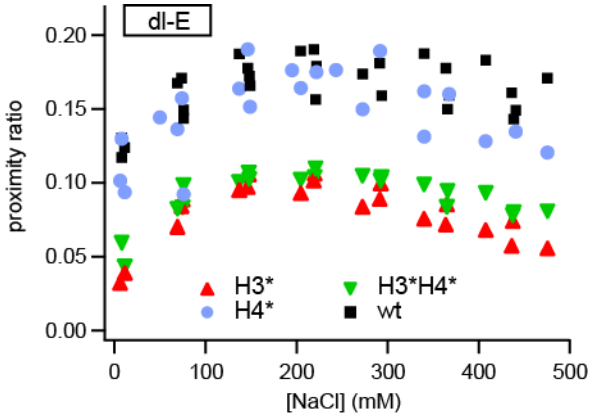

Figure S5

Electrophoretic mobility shift assay (EMSA) of acetylated nucleosomes after incubation at elevated ionic strength. **A**) non-acetylated, **B**) H3-acetylated, **C**) H4-acetylated and **D**) H3/H4-acetylated nucleosomes were incubated at 150, 600, 800 and 1000 mM NaCl. Changes in mobility were analyzed after 60 minutes incubation. All samples show conversion of nucleosomes into free DNA at higher ionic strength but no indication of salt-induced octamer repositioning along DNA.

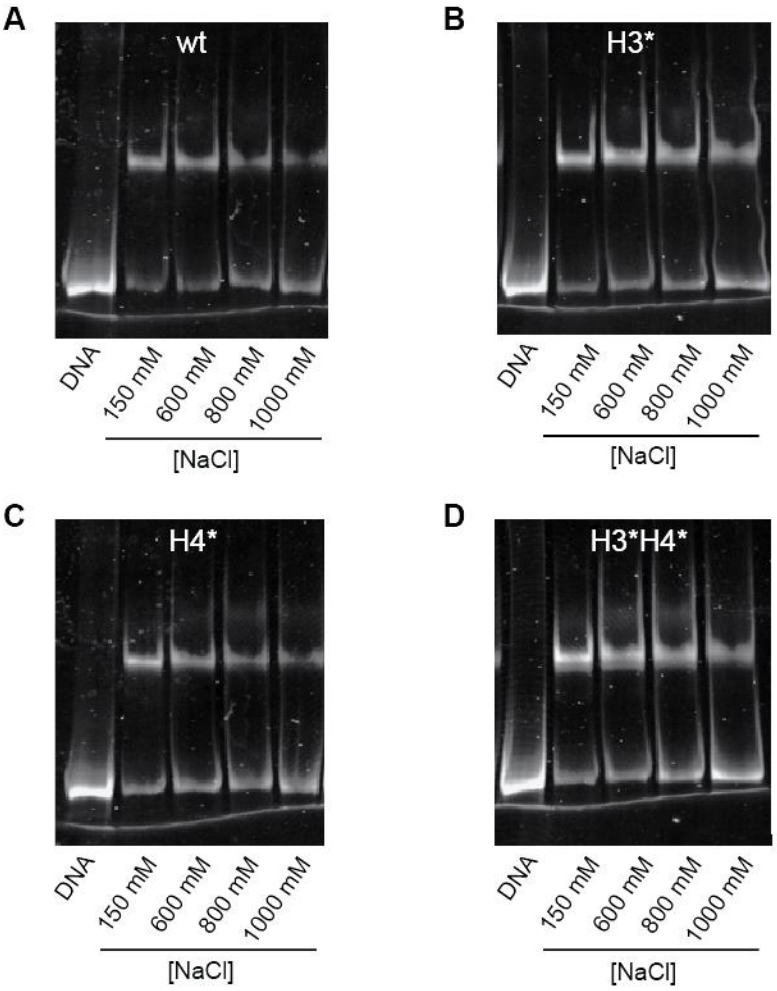

Figure S6

Comparison of non-acetylated nucleosomes (dark grey), H3*H4* nucleosomes (black) and nucleosomes with all histones acetylated (light gray): Additional acetylation of H2A and H2B caused a further increase in linker DNA unwrapping (by about 10%) but did not influence the salt concentration at which dl-I nucleosomes dissociated.

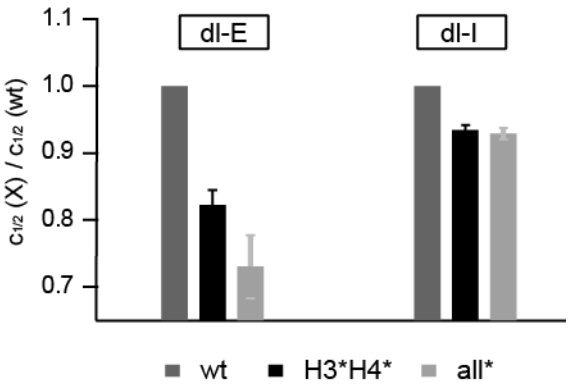

Figure S7

Simulation of distribution moments for a mixture of 2 FRET species (state A at P = 0.4 and state B at P = 0.55): (**A**) Exemplary distributions of 2000 events simulated for ratios A:B = 100:0, 75:25, 50:50, 25:75 and 0:100 (top to bottom). For illustration subpopulations are shown as Gaussians. **B-E**) Computed distribution moments (mean value (B), variance (C), skewness (D) and kurtosis (E)) as a function of state B abundance. A polynomial fit is shown as visual guidance. For each ratio A:B 10 individual distributions were simulated ; moments were computed for each simulated distribution and then averaged. Error bars represent the respective standard errors.

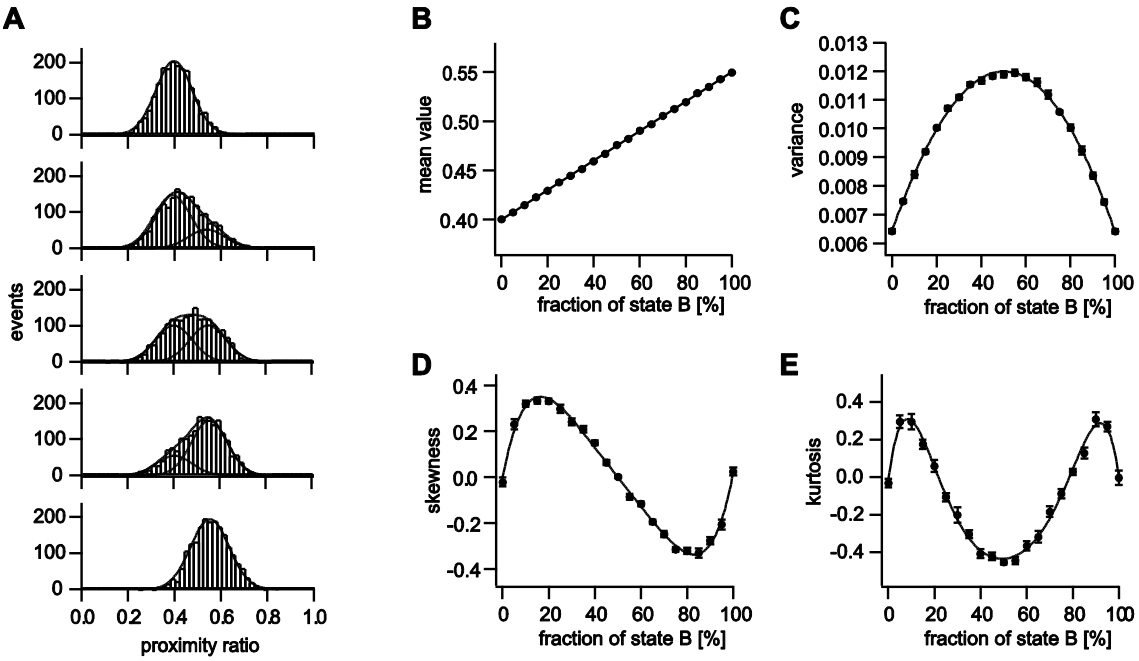

Figure S8

Distribution moment analysis of nucleosome spFRET data: (**A**) Exemplary spFRET distribution, relevant subpopulations of Donor-only, DNA and nucleosomes and computed weighting factor f used in the analysis of the FRET subpopulation P_{FRET}. Data are taken from H3-acetylated nucleosomes at 500 mM NaCl. (**B,C**) mean value and skewness of P_{FRET} as a function of salt concentration. (**D,E**) Sigmoidal fits to the rising and falling edge of the normalized and smoothed moments (box filter over the first adjacent neighbors). $c_{1/2}$ values from these fits are shown in manuscript Figure 4D.